RECENT MIGRATION RATES OF THE GREAT KOBUK SAND DUNES, ALASKA: TECHNOLOGIC AND SCIENTIFIC IMPLICATIONS FOR PLANETARY DUNE SYSTEMS.

M. Necsoiu[1] (mnecsoiu@swri.org), S. Leprince[2] , C. Dinwiddie[1], D. Hooper[1] and G. Walter[1]
[1]Geosciences and Engineering Division, Southwest Research Institute®, San Antonio, TX
[2]Division of Geological and Planetary Sciences, California Institute of Technology, Pasadena, CA.

Introduction: A novel method for precise orthorectification, coregistration, and subpixel correlation of SPOT and ASTER satellite imagery was applied to derive dune migration rates in a dune field in Kobuk Valley National Park, Alaska (Figure 1). This method corrects offsets due to sensor distortions and attitude drifts as well as orbital errors, providing a means for coregistering data with a 1/50 pixel accuracy. A 15-m-resolution digital elevation model (DEM) constructed from ASTER Stereo data was used in the orthorectification process. ASTER and SPOT datasets with a 5-year temporal separation were correlated to detect change and reveal lateral displacement. Despite a current lack of ground control for validation, confidence in remotely sensed velocity measurements was obtained through a series of tests including: visual inspection of the dune morphology with migration direction, and statistical tests, on and off the dune field, to quantify noise measurements and migration rate uncertainty.

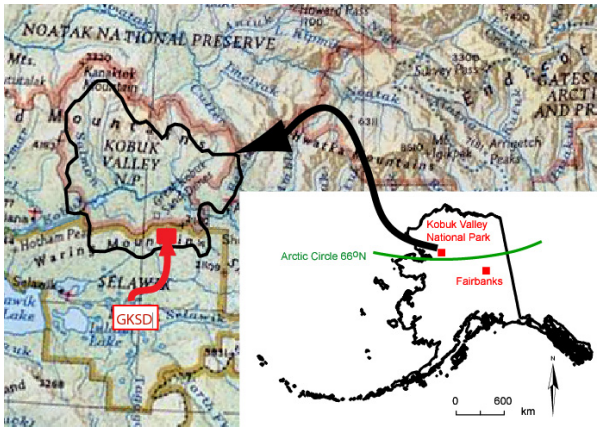

Figure 1. Geographical location of the Great Kobuk Sand Dunes within Kobuk Valley National Park (background image from Alaska Information Services).

Study Area: The Great Kobuk Sand Dunes (GKSD) occupy 62 km^2 in the central Kobuk River valley at 67° north latitude [1]. This active dune system is characterized by a variety of dune forms, including transverse, longitudinal, barchanoid, and coppice (nebkha) dunes and sand sheets [1,2,3]. Pleistocene glaciation in the Brooks Range produced glacial drift reworked by subsequent meltwater streams; these streams deposited quartzose-rich sand and silt along the axis of the Kobuk River valley concurrent with the last glacial advance {24 ka [3]} and created loess deposits and cold-climate dunefields. With the river valley axis oriented E–W, there exists an opposite, bimodal wind regime at the macroscale, whereby the dominant winds are strong polar easterlies approximately 9 months of the year (September–May) but the winds reverse during the summer [1]. The climate is subarctic and semiarid (mean annual air temperature: –6°C; average precipitation: 400 mm) with long, cold winters and brief warm summers [4,5,6]. The downwind side of GKSD is characterized by a main body of large transverse to barchanoid (arms pointing downwind to the west) dune ridges, longitudinal dunes, and flat interdune areas [3]. The main body of sand is dry and has a large sand supply [3,7]. Ferrians suggested that the valley is underlain by discontinuous permafrost in a narrow band immediately surrounding the river but is underlain to the north and south by continuous permafrost at moderately higher elevations including, notably, the area of the GKSD [8]. The potential presence of permafrost within the GKSD combined with the opposite, bimodal wind regime of Kobuk Valley likely leads to a lower than average dune migration rate [1,7], but migration rates for this dune field have not been estimated until now.

Remote Sensing Datasets: The operational use of the method presented here allows cross-correlation of images acquired by different imaging systems with different viewing angles, and without the need for information other than what is extracted from satellite ancillary data and topography. Optical datasets used in this study are listed in Table 1.

Table 1. Optical Datasets Used in this Study

Satellite Dataset Granule ID	Date	Viewing Angle	Orientation (degrees)
ASTER L1A#0030614200322253 0	6/14/2003	−0.025	21.2405
SPOT 5 L1A 421-210/6	8/7/2008	−15.41	18.7687

Methodology: We used the Coregistration of Optically Sensed Images and Correlation (COSI-Corr) method described by [9,10] to accurately orthorectify and coregister pairs of optically sensed images, irrespective of sensor type and resolution. Included in this method is a powerful correlation tool that enables measurement of horizontal E–W/N–S ground movement. The typical uncertainty on detected movement is on the order of 1/10 the nominal image pixel size. Satellite data were processed as follows [11]:

1. SPOT satellite data were orthorectified and georeferenced using metadata.dim information and a 15-m ASTER Stereo-based DEM.
2. Mapping matrices were computed and SPOT data were resampled to a ground resolution matching the ASTER image resolution (i.e., 15 m). A Sinc kernel improved resampling quality and ultimate correlation.
3. ASTER satellite data were orthorectifed by selecting 15 tie points between the ASTER image and the orthorectified SPOT image. These tie points were then converted to ground control points (GCP) and optimized. Three GCPs had high residual values and were eliminated. Mapping matrices to orthorectify the ASTER image were computed and the ASTER 3N band was resampled.
4. The two coregistered and orthorectified datasets were correlated to produce two displacement maps (i.e., E/W and N/S) and a signal to noise ratio image for assessing the quality of results.

Results: The correlation of ASTER and SPOT datasets with a 5-year temporal separation revealed displacements on the order of 2 m/yr (Figure 2). We derived 6 correlation-optimized ground control points with an average normalized mis-registration of 6.5 cm. *A posteriori* verification from the complete correlation data allows to conclude that the global registration of the images is better than 85cm. This potentially large registration error is to be regarded as an upper bound due to the large number of outliers in the correlation, which could not all be removed in the *a posteriori* statistics [11].

Previous studies highlighted potential problems when calculating the correlation for certain dataset pairs (e.g., for two ASTER images) [9,10]. Artifacts occur as waves of amplitude ~3–10 m, which are characteristic of attitude instabilities on ASTER's Terra platform. We did not observe this problem using these SPOT and ASTER datasets.

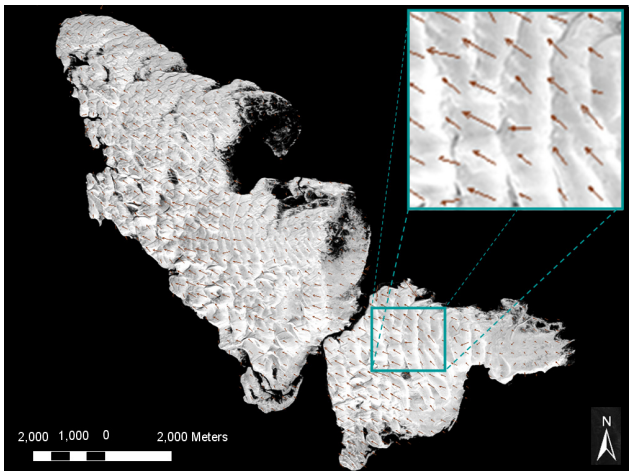

Figure 2. Sand Dune Migration. Vectors of movement are superimposed on the SPOT Panchromatic image.

Discussion: Sand dunes are common on Earth, Mars, and Titan. Actively migrating dunes have not yet been identified on Mars [12,13], but the shrinkage and disappearance of two dome dunes over a period of 3 Mars years suggests significant ongoing sand transport [14]. Bourke et al. [15] recently reported a Victoria Valley, Antarctica, estimate for migration rates of perennial niveo-aeolian transverse and barchan sand dunes. Using vertical air photos and a recent LIDAR dataset they estimated a 1.5 m/yr average dune migration rate with individual dunes having rates of 0.5 to 2.8 m/yr [15]. In contrast, niveo-aeolian deposits at the GKSD are ephemeral, disappearing each summer, which suggests they would play a lesser role in arresting dune movement; however, movement-limiting permafrost is suspected at depth within the GKSD [1,7]. Our average migration rate estimate for the GKSD is thus consistent with the Antarctica estimate given the relatively warmer subarctic, semiarid climate of the GKSD compared to the polar desert, hyperarid climate of the Victoria Valley dunes.

Uncertainty in our migration rate estimate will be significantly reduced when our team collects GCPs on the ground in 2010 with a differential global positioning system to verify the quality of our ASTER Stereo-based DEM. If available, a LIDAR-derived DEM of the GKSD would improve dune migration rate estimates even more.

Conclusions: The novel orthorectification, coregistration, and subpixel correlation method we applied here provides a fast and economically viable method to monitor active morphological processes on planetary surfaces and in remote terrestrial locales.

References: [1] Koster E.A. and Dijkmans J.W.A. (1988) *Earth Surface Processes and Landforms*, *13*, 153–170. [2] Fernald A.T. (1964) USGS 1181–K, k1–k31. [3] Dijkmans J. and Koster E. (1990) *Geofiska Annaler, 72A,* 93–109. [4] Leslie, L.D (1989) Arctic Environmental Information and Data Center, U. Alaska Anchorage. [5] Brabets, T.P. (2001) USGS WRIR 01–4141. [6] Harris, A.G. et al. (2004) *Geology of National Parks.* 6th Ed. Kendall/Hunt Pub. Co., Dubuque, IA. [7] Mann D.H. et al. (2002) *Quaternary Science Rev., 21,* 709–731. [8] Ferrians, O.J. (1965) USGS Misc. Geologic Investigations Map I-445. [9] Leprince S. et al. (2007) *IEEE Trans. Geosci. Remote Sens., 45,* 1529–1558. [10] Ayoub F. et al. (2008) Proc. *IGARSS*, Boston. [11] Necsoiu D.M. et al. (2009) *in preparation for the IEEE Geosci. and Remote Sens. Newsletter* [12] Zimbelman, J.R. (2000) *Geophys. Res. Lett., 27,* 1069–1072. [13] Schatz, V. et al. (2006) *JGR–Planets, 111,* 10.1029/2005JE002514. [14] Bourke, M.C. et al. (2008) *Geomorphology, 94,* 247–255. [15] Bourke M.C. et al. (2008) Planetary Dunes Workshop, Abstract #7040.

Acknowledgements: This research was funded through SwRI's internal research and development program through Quick-Look Project R8002: Kobuk Valley National Park Landscape Change Detection Using Remotely Sensed Data and Geomorphologic Assessments. S. Leprince was partially supported by the NSF grant EAR-0636097, and by the Gordon and Betty Moore Foundation.